Taming turbulence in the complex Ginzburg-Landau equation

Meng Zhan,[1,*] Wei Zou,[1,2] and Xu Liu[1,2]
[1]*Wuhan Institute of Physics and Mathematics, Chinese Academy of Sciences, Wuhan 430071, China*
[2]*Graduate School of the Chinese Academy of Sciences, Beijing 100049, China*
(Received 11 October 2009; published 10 March 2010)

Taming turbulence in the complex Ginzburg-Landau equation (CGLE) by using a global feedback control method and choosing traveling-wave solutions as our target state is investigated. The problem of *optimal control* for the smallest driving strength is studied by systematically comparing the stabilities of all traveling waves. Within the Benjamin-Feir-Newell unstable parameter region ($c_2<-c_1^{-1}$), a critical control curve is determined, which is located at $c_2=\alpha c_1^{\beta}$, with $\alpha\approx-4.0$ and $\beta\approx-0.87$. It characterizes the transition of chosen traveling-wave target state from long wavelength to short one. This finding is of great significance for taming turbulence in the CGLE and some other spatiotemporal systems as well.

DOI: 10.1103/PhysRevE.81.036211 PACS number(s): 05.45.Gg, 47.27.Rc

Chaos control with the aim to transform an original chaotic system to a regular state was pioneered by Ott, Grebogi, and Yorke (OGY) in 1990 [1]. Intuitively chaos is uncontrolled, due to the intrinsic feature of chaotic systems: the extreme sensitivity to tiny perturbations. Their innovative work, however, demonstrated that chaos is controllable, if one properly chooses small disturbances of chaotic system, which stabilize the system in the neighborhood of a desirable unstable periodic orbit naturally embedded in the chaotic motion. In this respect, the chaotic system embedded with infinite unstable periodic orbits serves as a reservoir of rich information, and we have benefited from this for the controllability, efficiency, and flexibility in the control [1,2]. Later on, Pyragas proposed a time-delayed feedback control method to self-search the most stable periodic orbit [3]. After the success of chaos control in low-dimensional nonlinear systems, the general interest of researchers has shifted to the control of spatially extended systems [4–9]. So far, various control approaches have been proposed, including the local pinning control [10–12], the time-delayed feedback control [13,14], the adaptive method [15] and the forcing in Fourier space [16], and in wavelet subspace [17]. Driven by the strong motive force of practical applications, the control of spatiotemporal chaos remains a great challenge in the field of nonlinear science. For recent developments, see the review papers [18].

In this work, we generalize the basic idea of OGY method to the control of spatiotemporal chaos. In the spatially extended systems, all the traveling-wave solutions (namely, the spatiotemporal periodic states) that are unstable can be viewed as being embedded in the turbulent state, similar to the unstable periodic orbits embedded in the temporal chaotic attractor. Using a global feedback control method and analyzing their stabilities of all the traveling-wave solutions against all external perturbations, we may choose the least unstable one and achieve the best control efficiency.

As an example, we study the following one-dimensional complex Ginzburg-Landau equation (CGLE) [19]:

$$\partial_t A = A + (1+ic_1)\partial_x^2 A - (1+ic_2)|A|^2 A, \tag{1}$$

where $A=A(x,t)$ is complex and c_1 and c_2 are (real) system parameters. The CGLE has been extensively studied for the problems of pattern formations, turbulence, and chaos control. With the periodic boundary condition $A(x+L,t)=A(x,t)$, the system (1) has the following traveling-wave solutions:

$$A(x,t) = A_0 e^{i(kx-wt)}, \tag{2}$$

with $A_0=\sqrt{1-k^2}(0\le k\le 1)$ and $w=c_2+(c_1-c_2)k^2$. $k(k=1/\lambda)$ and w are the wave number and rotation frequency, respectively. Since both the amplitude A_0 and frequency w are determined by the wave number k, $k(0\le k\le 1)$ can be viewed as only one tunable parameter.

The stability of the traveling-wave solutions has been well analyzed by performing the linear stability analysis and reported in the literature [18–21], which shows that it is governed by the sign of the real part of the following eigenvalue:

$$\sigma = \frac{1}{2}(F_{11}+F_{22}) + \frac{1}{2}\sqrt{(F_{11}-F_{22})^2+4F_{12}F_{21}} \tag{3}$$

with

$$F_{11} = -p^2 - i2kc_1p - 2(1-k^2),$$

$$F_{12} = c_1p^2 - i2kp,$$

$$F_{21} = -c_1p^2 + i2kp - 2c_2(1-k^2),$$

$$F_{22} = -p^2 - i2kc_1p.$$

Here, $p(0\le p\le 1)$ stands for the wave number of perturbations. An instability occurs if $\mathrm{Re}[\sigma(k,p)]>0$.

Expansion of σ for general k but small $p(p\ll 1)$ to second order in p yields

$$\mathrm{Re}(\sigma) = -\left(1+c_1c_2-2k^2\frac{1+c_2^2}{1-k^2}\right)p^2. \tag{4}$$

Thus, these traveling-wave solutions are linearly stable against long-wavelength perturbations if

*Corresponding author; zhanmeng@wipm.ac.cn

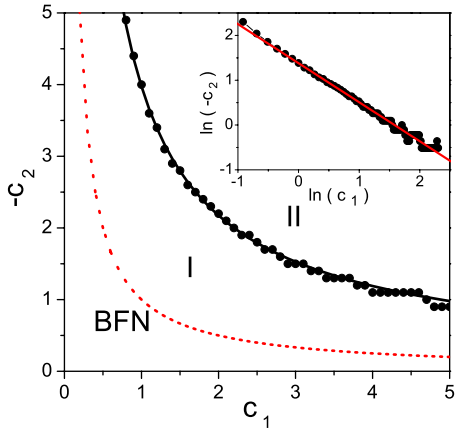

FIG. 1. (Color online) The two critical curves in the $(c_1,-c_2)$ parameter space: one is the Benjamin-Feir-Newell curve (dashed line, denoted by the letters "BFN") characterizing the stability-instability transition of traveling waves, $c_2=-c_1^{-1}$, and the other is the critical control curve (solid line) characterizing the transition of chosen traveling wave as target state from long wavelength ($k=0$) to short one ($k\approx 1$), $c_2=\alpha c_1^{\beta}$, with $\alpha\approx -4.0$ and $\beta\approx -0.87$. The inset shows the fit in the log-log plot.

$$k^2 < k_E^2 = \frac{1+c_1c_2}{2(1+c_2^2)+1+c_1c_2} \tag{5}$$

holds. Further, we have if $1+c_1c_2<0$ [the so-called Benjamin-Feir-Newell (BFN) unstable region], all traveling-wave solutions are unstable and various spatiotemporal turbulent behaviors are possible. For illustration, we plot the BFN critical curve ($c_1c_2=-1$) in the $(c_1,-c_2)$ parameter space in Fig. 1. For more details about the phase diagram of CGLE exhibiting phase turbulence, defect turbulence, bichaos, and intermittent behaviors, see Refs. [21–23].

We use a global feedback control approach by injecting a periodic signal into the original system and change Eq. (1) to the controlled form

$$\partial_t A = A + (1+ic_1)\partial_x^2 A - (1+ic_2)|A|^2 A + \varepsilon(\hat{A}-A), \tag{6}$$

with ε the feedback control strength and $\hat{A}$ the target state chosen from one of the periodic traveling waves of Eq. (2). In contrast to our global feedback control approach, Boccaletti *et al.* [24,25] have theoretically studied the control and synchronization of the CGLE with the same feedback form but by means of a finite number of local perturbations (the so-called local feedback control approach). In the absence of the feedback term in Eq. (6), the dynamical response of patterns to a direct spatiotemporal forcing in the form of a traveling-wave modulation of a control parameter has also been studied and observed in the reaction-diffusion experimental systems [26–28]. Thus, we expect that the model equation Eq. (6) is not only a mathematical model, but also plausible physically.

As $A=\hat{A}$ is already a solution of controlled system [Eq. (6)], the effect of control simply changes the stability of the solution-from unstable to stable. Again performing the linear stability analysis with respect to the target state, we obtain that the critical control strength ε_c should be equal to $\mathrm{Re}(\sigma)$ of single traveling wave, namely,

$$\varepsilon_c = \mathrm{Re}(\sigma). \tag{7}$$

For the detailed derivation, see our recent work in Ref. [29]. This equality clearly indicates that the controllable condition is determined by the degree of stability of single traveling wave.

Consequently, the problem of the smallest control intensity for the best control efficiency becomes how to choose the least unstable traveling-wave solution among all the unstable solutions that embedded in the turbulent motion. Here, we assume that all solutions (2) can be freely chosen. For this purpose, the stabilities of all traveling-wave solutions have to be compared and the least unstable one should be picked. This is similar to the manipulation in the OGY control method, in which some of the unstable low-period periodic orbits that are embedded in the chaotic attractor are chosen. Clearly, they are the least unstable ones and can be more easily found. Here, it also should be mentioned that in the traditional stability analysis, this comparison is unnecessary, as the traveling waves are all unstable in the turbulent state. In the control, however, such a comparison based on Eqs. (3) and (7) is not only necessary but also important.

Our main result is the finding of a critical curve for the control

$$c_2 = \alpha c_1^{\beta} \tag{8}$$

with $\alpha\approx -4.0$ and $\beta\approx -0.87$. The power law relation can be seen from a perfect log-log fit in the inset in Fig. 1. In contrast to the traditional BFN line (dashed line) for the change in stability of traveling-wave solutions, the critical control line (solid line) is for the choosing of wave number in the control problem. It divides the whole BFN unstable parameter region into two separated parts, region I and region II, as shown in Fig. 1; in region I (II), the longest (short) wavelength $k=0(k\approx 1)$ should be chosen for the best control efficiency. Within the BFN stable region, as some of traveling waves are already stable, no control is needed. This classification is apparently of great significance and is expected to be generalized to other complex systems.

From the knowledge of the linear stability analysis of traveling waves [Eqs. (3)–(5)], we already know that the long-wavelength traveling waves are important, and especially the longest ($k=0$) is the last one losing its stability and plays a crucial role. Consequently, the BFN line signals the change in its stability and further the division of regular and irregular motions in the phase diagram. Our study reveals that the parameter regime of the $k=0$ traveling wave being the most stable actually can be extended to the whole region I (see Fig. 1) and thus a critical control curve exists for the division of the choosing of the longest wavelength and the short one.

Below we analyze $\varepsilon_c(k,p)$ for $k=0$ and $k=1$. Inputting $k=0$ into Eq. (3) and considering Eq. (7), we obtain

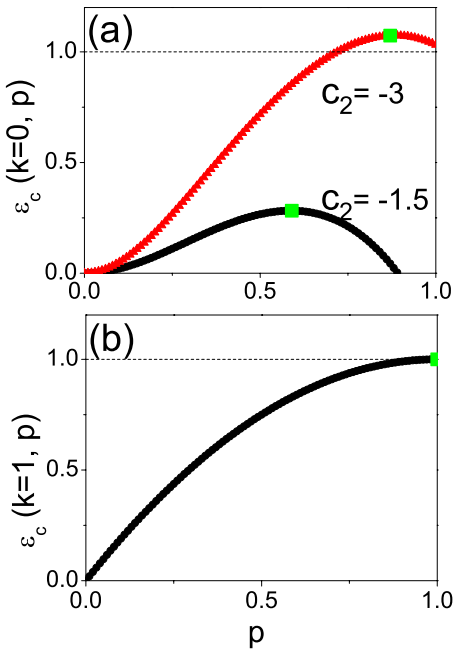

FIG. 2. (Color online) (a) and (b) The plots of $\varepsilon_c(k,p)$ vs p for $k=0$ and $k=1$, respectively. The value of $\varepsilon_c(k,p)$ for $k=0(k=1)$ is dependent (independent) of the parameters c_1 and c_2. In (a), $c_1=2.1$; $\varepsilon_c(k=0,p)$ monotonically increases with decrease of c_2. In both panels, the maximum of curve is highlighted by a square.

$$\varepsilon_c(k=0,p) = -p^2 - 1 + \sqrt{1 - c_1 p^2 (c_1 p^2 + 2c_2)}. \quad (9)$$

The $\varepsilon_c(k=0,p)$ as a function of p is plotted in Fig. 2(a) for two different parameters: $c_2=-1.5$ within the region I (the long-wavelength region) and $c_2=-3.0$ within the region II (the short wavelength region). $c_1=2.1$ is fixed. For a successful control, the wave has to be stable against all external perturbations. For the consideration of physical meaning, p can only be changed between 0 and 1. We find that the value of $\varepsilon_c(k=0,p)$ and further the maximum value get larger for a smaller c_2 (comparing the two lines); this point can be easily analyzed by Eq. (9). The maximum value for $c_2=-3.0$ is already larger than 1 and for a smaller c_2 it can get much larger. In this figure, the peak of each curve is highlighted by a square.

On the other hand, the traveling wave with the shortest wavelength $(k=1)$ corresponds to a homogeneous steady state, $A=0$. Now inputting $k=1$ into Eq. (3) and considering Eq. (7), we have

$$\varepsilon_c(k=1,p) = -p^2 + 2p. \quad (10)$$

This parabolic function is plotted in Fig. 2(b), showing a peak value $\varepsilon_c(k=1)=1$ at $p=1$, which indicates that the critical control strength ε_c for $k=1$ is always fixed and equals 1. Clearly, this relation $\varepsilon_c(k=1)=1$ is independent of any c_1 and c_2, and it actually sets an upper bounded condition for all controls.

Except for these two extremes, an analysis of the stability (or, equivalently, the critical control strength) for all wave numbers of the basic states k and the perturbations p in Eq. (3) is impossible, and we have to rely on numerical simulations. As the first step, we calculated the distribution of $\varepsilon_c(k,p)$ with the variations of k and p for all c_1 and c_2. For illustration, the results for the two different parameters: $c_2=-1.5$ and $c_2=-3.0$, are shown in Figs. 3(a) and 3(b), respectively. $c_1=2.1$ is unchanged. Both k and p are tuned from 0 to 1. Comparing these two panels, we immediately find that the pattern in Fig. 3(b) substantially changes with the occurrence of a new saddle at large k (indicated by the arrow). Meanwhile, the slope at the small k region is greatly lifted and the value around $k=1$ is nearly unchanged. These pattern changes definitely give rise to the change in the chosen target state for the best control efficiency, as we will see below.

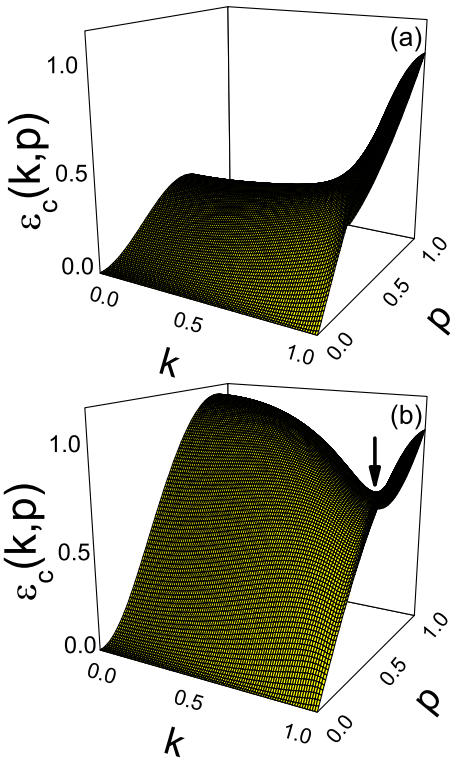

FIG. 3. (Color online) The plots of $\varepsilon_c(k,p)$ vs k and p for the different parameters: (a) $c_2=-1.5$ within the region I in Fig. 1, and (b) $c_2=-3.0$ within the region II. $c_1=2.1$. The curves for $k=0$ (the leftmost) and $k=1$ (the rightmost), as shown in Fig. 2, are clear. In (b), the saddle located at large k and large p is emphasized by an arrow.

The same as the analysis for $k=0$ and $k=1$, to warrant a successful control, we have to choose the maximum of $\varepsilon_c(k,p)$, $\varepsilon_c(k)=\mathrm{Max}\{\varepsilon_c(k,p), 0\le p\le 1\}$, for a certain k. To obtain the highest control efficiency, we need to further choose the minimum of $\varepsilon_c(k)$, $\varepsilon_c=\mathrm{Min}\{\varepsilon_c(k), 0\le k\le 1\}$. The corresponding k is denoted by k_c. For illustration, the dependence of $\varepsilon_c(k)$ on k for different c_2's is shown in Fig. 4. $c_1=2.1$ is fixed. For the parameter within the BFN stable region, the critical wave number k_E corresponding to the transition of $\varepsilon_c(k)$ from zero to positive can be well predicted by Eq. (5). See, e.g., $c_2=0$ and $k_E\approx 0.58$. For $c_2=-0.48\approx -1/c_1$ (the dashed line in the figure), $\varepsilon_c(k)$ monotonically increases from the origin $\varepsilon_c(k=0)=0$. As c_2 decreases further, e.g., $c_2=-1.0$ within the region I in Fig. 1, the monotonic increasing of $\varepsilon_c(k)$ with k persists but $\varepsilon_c(k=0)$ begins

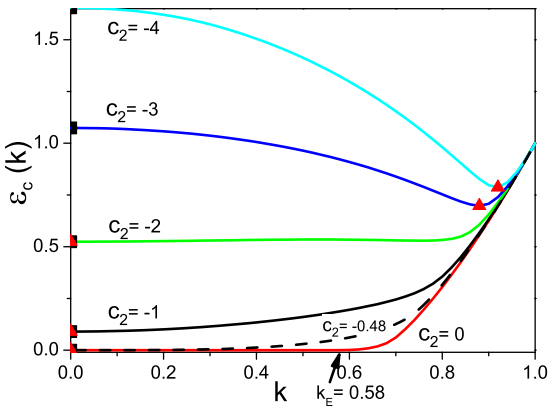

FIG. 4. (Color online) The plots of $\varepsilon_c(k)$ vs k for different c_2's. From top to bottom, $c_2=-4,-3,-2,-1,-0.48$ (dashed line), and 0. $c_1=2.1$. The points of $\varepsilon_c(k)$ for $k=0$ and the minimum points of $\varepsilon_c(k)$ for $0\leq k\leq 1$ for these parameters are indicated by squares and triangles, respectively.

to be positive. Under this situation, a feedback control on the longest-wavelength wave ($k=0$), which keeps the most stable, has to be applied for the smallest control strength. This pattern changes if c_2 decreases further and moves across the critical control line into region II. See, e.g., $c_2=-3$ and -4. The minimum point of $\varepsilon_c(k)$ has suddenly shifted from $k=0$ (square) to $k\approx 1$ (triangle). For the parameter within region II, however, the value of k_c is only slightly changed (comparing the two curves for $c_2=-3$ and -4). At the exact critical parameter ($c_2=-2$), the critical behavior with a plateau at $0\leq k\leq 0.8$ is clear. The reason for this change in pattern obviously comes from two opposite effects: one is the increase of $\varepsilon_c(k)$ for $k=0$ for smaller c_2 and the other is the identity of $\varepsilon_c(k)$ for $k=1$ for all parameters. Both effects have been well analyzed in Eqs. (9) and (10) and illustrated in Fig. 2.

Finally, the minimum data of the $k-\varepsilon_c(k)$ curve for all parameters c_1 and c_2 are selected, and the corresponding ε_c and k_c are plotted in Figs. 5(a) and 5(b), respectively. The big jump from zero (one plateau) to positive (the other plateau) of ε_c for the parameters (c_1,c_2) from the BFN stable to unstable region and that of k_c from region I to region II are clear. Both ε_c and k_c are bounded ($\varepsilon_c<1$ and $k_c<1$) according to the stability analysis of the shortest-wavelength plane wave above. These figures could guide us to choose target state properly and are apparently of significance.

All the above analyses and predictions have been verified by numerical simulations. For instance, Figs. 6(a) and 6(b) show the different control results for $\varepsilon=0.72>\varepsilon_c$ and $\varepsilon=0.6<\varepsilon_c$, respectively. $\varepsilon_c=0.70$. $c_1=2.1$ and $c_2=-3.0$. A traveling wave of wave number k close to $k_c(k_c\approx 0.88)$ is chosen as target state. In sharp contrast to the elimination of the defect turbulent behavior in Fig. 6(a), the irregularity after control is discernible in Fig. 6(b).

In summary, we have simply used inherent system's information (the unstable traveling-wave solution) to the control of turbulence, and studied the problem of the smallest control strength for the highest control efficiency. A critical curve for the control is unveiled. Our study shows that one has to properly choose traveling waves as target state. In

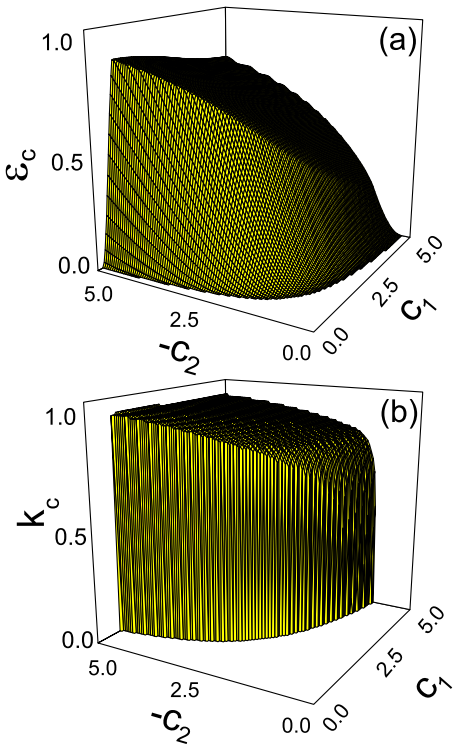

FIG. 5. (Color online) The critical control strength ε_c (a) and the corresponding wave number k_c (b) plotted vs c_1 and $-c_2$. The transition loci from zero to positive value of ε_c in (a) and k_c in (b) correspond to the BFN critical stability curve and the critical control curve in Fig. 1, respectively.

particular, traveling waves with either the long wavelength or the short wavelength in the different parameter regions (region I or II) should be correctly chosen. Below, it is worthwhile to give some discussions. (a) Recently, researchers have revealed that the spatiotemporal chaoticity monotonically increases with increase in the absolute values of c_1 and c_2 within the BFN unstable region by the calculations of both the largest Lyapunov exponent and the number of positive

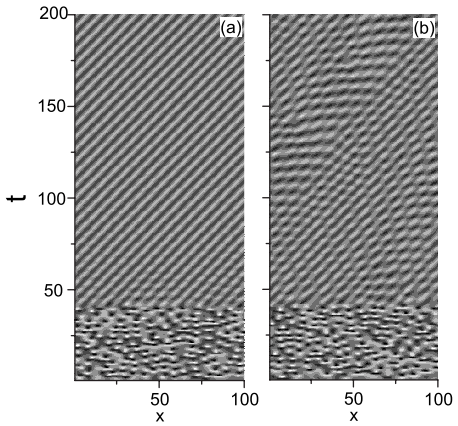

FIG. 6. (a) and (b) The time evolutions of Re$[A(x,t)]$ with a traveling-wave solution globally applied for $\varepsilon=0.72>\varepsilon_c(\varepsilon_c=0.70)$ and $\varepsilon=0.6<\varepsilon_c$, respectively, to show the different control results. The control is switched on at $t=40.0$. $c_1=2.1$ and $c_2=-3.0$. $L=100$, $m=14$, and $k=\frac{2\pi m}{L}\approx k_c=0.88$ are chosen.

Lyapunov exponents [10]. Thus, one may intuitively believe that the turbulent state becomes more difficult to be controlled for the parameter set (c_1, c_2) chosen deeper into the BFN unstable region. Our control result in Fig. 5 with a finite control strength $\varepsilon_c < 1$ for any c_1 and c_2 is clearly contrary to this intuitive idea and exhibits a strikingly high efficiency. (b) Our control method in Eq. (6) is a global one, as the traveling-wave perturbations in the feedback term have to be applied at any point of the systems. But the control effect is a local one, as our method still uses the classical linearization method to control unstable states in the system. Usually, initial conditions very close to the target traveling-wave solution have to be chosen; the peculiar effect of initial conditions on the control effect has been studied in our recent work [29]. In contrast to this, recently, Waleffe and coworkers [8] studied the topology of turbulence and its use for control. It is truly nonlinear and does not rely on local linear perturbations to local states. (c) Although our work is motivated by the classical OGY method, their difference is clear. (d) Our recent work also showed the important impact of a spatial-locally applied shortest-wavelength wave $(A=0)$ in the control of two-dimensional turbulence [30]. Therefore, the feedback method forced by a homogeneous steady state may become an excellent candidate in the control of strong turbulence for its simplicity and efficiency. (e) Finally, as the CGLE is capable of providing a qualitative and even a quantitative description for a vast variety of phenomena, we expect the control method and the results can be applied and generalized to other spatiotemporal systems.

This work was supported by the Outstanding Oversea Scholar Foundation of Chinese Academy of Sciences (Bairenjihua).

[1] E. Ott, C. Grebogi, and J. A. Yorke, Phys. Rev. Lett. **64**, 1196 (1990).
[2] T. Shinbrot, C. Grebogi, E. Ott, and J. A. Yorke, Nature (London) **363**, 411 (1993).
[3] K. Pyragas, Phys. Lett. A **170**, 421 (1992).
[4] G. Franceschini, S. Bose, and E. Scholl, Phys. Rev. E **60**, 5426 (1999).
[5] J. Bragard and S. Boccaletti, Phys. Rev. E **62**, 6346 (2000).
[6] S. G. Guan, Y. C. Zhou, G. W. Wei, and C.-H. Lai, Chaos **13**, 64 (2003).
[7] S. G. Guan, G. W. Wei, and C.-H. Lai, Phys. Rev. E **69**, 066214 (2004).
[8] J. Wang, J. Gibson, and F. Waleffe, Phys. Rev. Lett. **98**, 204501 (2007).
[9] A. Ahlborn and U. Parlitz, Phys. Rev. E **77**, 016201 (2008).
[10] J. H. Xiao, G. Hu, J. Z. Yang, and J. H. Gao, Phys. Rev. Lett. **81**, 5552 (1998).
[11] L. Junge and U. Parlitz, Phys. Rev. E **61**, 3736 (2000).
[12] C. Mendoza, J. Bragard, P. L. Ramazza, J. Martinez-Mardones, and S. Boccaletti, Math. Biosci. Eng. **4**, 523 (2007).
[13] M. E. Bleich and J. E. S. Socolar, Phys. Rev. E **54**, R17 (1996); W. Just, T. Bernard, M. Ostheimer, E. Reibold, and H. Benner, Phys. Rev. Lett. **78**, 203 (1997).
[14] M. Bertram and A. S. Mikhailov, Phys. Rev. E **63**, 066102 (2001).
[15] S. Sinha and N. Gupte, Phys. Rev. E **58**, R5221 (1998).
[16] S. J. Jensen, M. Schwab, and C. Denz, Phys. Rev. Lett. **81**, 1614 (1998).
[17] G. W. Wei, M. Zhan, and C.-H. Lai, Phys. Rev. Lett. **89**, 284103 (2002).
[18] S. Boccaletti, C. Grebogi, Y.-C. Lai, H. Mancini, and D. Maza, Phys. Rep. **329**, 103 (2000); M. Ipsen, L. Kramer, and P. G. Sørensen, *ibid.* **337**, 193 (2000); A. S. Mikhailov and K. Showalter, *ibid.* **425**, 79 (2006); G. Rega and S. Lenci, Philos. Trans. R. Soc. London, Ser. A **364**, 2269 (2006); *Handbook of Chaos Control*, 2nd ed. edited by E. Schöll and H. G. Schuster (Wiley-VCH, Weinheim, 2008) (and references therein).
[19] Y. Kuramoto, *Chemical Oscillations, Waves, and Turbulence* (Springer, Berlin, 1984).
[20] B. Janiaud, A. Pumir, D. Bensimon, V. Croquette, H. Richter, and L. Kramer, Physica D **55**, 269 (1992).
[21] I. Aranson and L. Kramer, Rev. Mod. Phys. **74**, 99 (2002).
[22] B. I. Shraiman, A. Pumir, W. van Saarloos, P. C. Hohenberg, H. Chate, and M. Holen, Physica D **57**, 241 (1992).
[23] H. Chate, Nonlinearity **7**, 185 (1994).
[24] S. Boccaletti, J. Bragard, and F. T. Arecchi, Phys. Rev. E **59**, 6574 (1999).
[25] S. Boccaletti and J. Bragard, Philos. Trans. R. Soc. London, Ser. A **364**, 2383 (2006).
[26] S. Rüdiger, D. G. Míguez, A. P. Muñuzuri, F. Sagués, and J. Casademunt, Phys. Rev. Lett. **90**, 128301 (2003).
[27] D. G. Míguez, V. Pérez-Villar, and A. P. Muñuzuri, Phys. Rev. E **71**, 066217 (2005).
[28] I. R. Epstein, I. B. Berenstein, M. Dolnik, V. K. Vanag, L. Yang, and A. M. Zhabotinsky, Philos. Trans. R. Soc. London, Ser. A **366**, 397 (2008).
[29] J. H. Gao, L. L. Xie, W. Zou, and M. Zhan, Phys. Rev. E **79**, 056214 (2009).
[30] J. H. Gao and M. Zhan, Phys. Lett. A **371**, 96 (2007).